Institute for Advanced Simulation

Density Functional Theory and Linear Scaling

Rudolf Zeller

published in

Multiscale Simulation Methods in Molecular Sciences,
J. Grotendorst, N. Attig, S. Blügel, D. Marx (Eds.),
Institute for Advanced Simulation, Forschungszentrum Jülich,
NIC Series, Vol. **42**, ISBN 978-3-9810843-8-2, pp. 121-144, 2009.

http://www.fz-juelich.de/nic-series/volume42

Density Functional Theory and Linear Scaling

Rudolf Zeller

Institute for Solid State Research and Institute for Advanced Simulation
Forschungszentrum Jülich, 52425 Jülich, Germany
E-mail: ru.zeller@fz-juelich.de

The basic concepts of density functional theory and of linear-scaling techniques to solve the density functional equations are introduced. The Hohenberg-Kohn theorem, the one-to-one mapping to an auxiliary non-interacting electron system to obtain the single-particle Kohn-Sham equations, and the construction of approximations for the exchange-correlation functional are explained. The principle of nearsightedness of electronic matter and its importance to achieve linear scaling are discussed. Finally, a recently in Jülich developed linear-scaling algorithm for metallic systems is presented and its suitability for large supercell calculations is illustrated.

1 Introduction

In the last decades density functional theory has emerged as a powerful tool for the quantum mechanical description of chemical and physical properties of materials. Density functional theory is an approach to treat the many-electron problem by single-particle equations. Instead of the many-electron wavefunction, which depends on $3N$ electronic space coordinates and N spin variables (here N is the number of electrons in the considered system), the basic quantity in density functional theory is the electron density $n(\underline{r})$, which depends on only three space coordinates. This obviously represents a considerable simplification for calculating, understanding and predicting material properties. The idea to use the density instead of the many-electron wavefunction was proposed by Thomas[1] and Fermi[2] already in 1927. The idea was fundamentally justified by the theorem of Hohenberg and Kohn[3] in 1964, which states that the ground-state energy of the many-electron system is uniquely determined by the ground-state density $n_0(\underline{r})$. Modern density functional theory has motivated an enormous number of applications primarily in the electron theory of atoms, molecules and solids, but density functional theory can be used also in the physics of liquids[4] and in nuclear physics[5].

However, although density functional theory accomplishes a considerable simplification, calculations for systems with many atoms still represent a serious computational challenge even after decades of effort to develop and improve computational techniques for the solution of the density functional equations. Systems with up to a few hundred atoms can be treated routinely today, but systems with thousands of atoms require overwhelming computing effort, because the computing time increases cubically with system size. In the last decade considerable work has been done to reduce the computational effort and linear scaling techniques have emerged as an approach to treat large systems with almost similar accuracy as available in standard techniques with cubic scaling.

The plan of this lecture is to introduce the concepts of density functional theory, to explain the reasons why linear scaling should be possible, to present the ideas used in several linear scaling techniques and finally to present an algorithm for metallic systems which was recently developed in our institute.

2 Density Functional Theory

To simplify the discussion[a] the consideration will be restricted here to a non-relativistic, non-spin-polarized, time-independent many-electron system moving in a potential provided by the electrostatic Coulomb interaction with atomic nuclei assumed at fixed positions. For this system the Hamilton operator $\hat{H}$ is given by a sum of the kinetic energy and the electron-electron, electron-nuclear and nuclear-nuclear interaction terms. Under the assumption that the nuclei are fixed the many-electron Schrödinger equation for N electrons is given by

$$\hat{H}\Psi = \left[-\frac{\hbar^2}{2m} \sum_i^N \nabla_i^2 + \sum_{i<j}^N \sum U(\underline{r}_i, \underline{r}_j) + \sum_i^N v_{ext}(\underline{r}_i) \right] \Psi = E\Psi, \qquad (1)$$

where $U(\underline{r}, \underline{r}') = e^2 |\underline{r} - \underline{r}'|^{-1}$ is the electron-electron interaction and $v_{ext}(\underline{r})$ the external potential, which contains the static potential arising from the interaction of the electrons with the nuclei and a constant term arising from the nuclear-nuclear interaction. Extensions of density functional theory to non-degenerate ground states, to spin-polarized and relativistic systems, to excited states and finite temperatures, to time-dependent and to superconducting situations are possible and can be found in the literature. Here, due to limited space, a discussion of these extensions is not possible.

2.1 Hohenberg-Kohn Theorem

The formal solution of the many-electron Schrödinger equation (1) defines a mapping from the external potential to the many-electron wavefunctions and thus also a mapping from external potential to the ground state wavefunction Ψ_0 and to the ground-state density $n_0(\underline{r})$. The first part of the Hohenberg-Kohn theorem states that the mapping can be inverted so that the external potential is uniquely determined by the ground-state density except for a trivial additive constant shift of the external potential. Because of the mapping from the ground-state density to the external potential and of the mapping from the external potential to the many-electron wavefunctions, there is also a mapping from the ground-state density to the many-electron wavefunctions and to every expectation value $\langle \Psi | \hat{O} | \Psi \rangle$, which means that every quantum mechanical observable is uniquely determined as a functional[b] of the ground-state density. The second part of the Hohenberg-Kohn theorem states that the total energy functional $E[n(\underline{r})]$ is minimal, if $n(\underline{r})$ is the ground-state density $n_0(\underline{r})$, and that the minimum $E_0 = E[n_0(\underline{r})]$ is the ground-state energy.

The proof of the Hohenberg-Kohn theorem for non-degenerate ground states proceeds by reductio ad absurdum and requires two steps. First it is shown that two potentials v_{ext} and v'_{ext}, which differ by more than a trivial constant $v_{ext} \neq v'_{ext} + const$, cannot lead to the same ground-state wavefunction Ψ_0 and then it is shown that two different ground-state wavefunctions Ψ_0 and Ψ'_0 (arising from two different potentials $v_{ext} \neq v'_{ext} + const$) cannot lead to the same ground-state density $n_0(\underline{r})$.

[a] This discussion is partly based on a previous article published in Lecture Manuscripts of the 37^{th} Spring School of the Institute of Solid State Research [6].

[b] Compared to a function $f(x)$, which is defined as a mapping from a variable x to a number f, a functional $F[f(x)]$ is defined as a mapping from a function $f(x)$ to a number F.

If one assumes that two potentials v_{ext} and v'_{ext}, which differ by more than a constant, lead to the same ground-state wavefunction Ψ_0, the subtraction of the Schrödinger equations for v_{ext} and v'_{ext} gives

$$(v_{ext} - v'_{ext})|\Psi_0\rangle = (E - E')|\Psi_0\rangle \; . \tag{2}$$

In regions with $\Psi_0 \neq 0$ the constant value $E - E'$ implies that the two potentials v_{ext} and v'_{ext} can differ only by a constant. Thus the assumption that v_{ext} and v'_{ext} differ by more than a constant can only be satisfied in regions where Ψ_0 vanishes. However, regions (with nonzero measure), where Ψ_0 vanishes, cannot exist because the unique continuation theorem[7,8] states that Ψ_0 vanishes everywhere if Ψ_0 vanishes in a region of nonzero measure. Thus the assumption that two potentials v_{ext} and v'_{ext}, which differ by more than a constant, lead to the same ground-state wavefunction requires that this wavefunction vanishes everywhere which is clearly impossible.

If one assumes that two different (apart from a trivial phase factor) ground-state wavefunctions Ψ_0 and Ψ'_0 for the different potentials v_{ext} and v'_{ext} lead to the same ground-state density $n_0(\underline{r})$, one obtains (see appendix)

$$\langle \Psi'_0 | v_{ext} - v'_{ext} | \Psi'_0 \rangle = \int n_0(\underline{r})[v_{ext}(\underline{r}) - v'_{ext}(\underline{r})]\mathrm{d}\underline{r} \tag{3}$$

and

$$\langle \Psi_0 | v'_{ext} - v_{ext} | \Psi_0 \rangle = \int n_0(\underline{r})[v'_{ext}(\underline{r}) - v_{ext}(\underline{r})]\mathrm{d}\underline{r} \; . \tag{4}$$

From $\langle \Psi_0 | \hat{H}_{v'} | \Psi_0 \rangle > \langle \Psi'_0 | \hat{H}_{v'} | \Psi'_0 \rangle = E'_0$, where the strict larger sign arises because Ψ'_0 is the ground-state wavefunction for the Hamiltonian $\hat{H}_{v'}$ which leads to the the ground-state energy ${E_0}'$, whereas Ψ_0, which differs from Ψ'_0 by more than a trivial phase factor leads to a larger energy, and from $\langle \Psi'_0 | \hat{H}_v | \Psi'_0 \rangle > \langle \Psi_0 | \hat{H}_v | \Psi_0 \rangle = E_0$, where the strict larger sign arises using similar arguments, one obtains

$$\langle \Psi_0 | \hat{H}_{v'} | \Psi_0 \rangle + \langle {\Psi_0}' | \hat{H}_v | {\Psi_0}' \rangle > E'_0 + E_0 \; . \tag{5}$$

Here the substitution $\hat{H}_{v'} = \hat{H}_v + v'_{ext} - v_{ext}$ in the first term and $\hat{H}_v = \hat{H}_{v'} + v_{ext} - v'_{ext}$ in the second term and the use of $\langle \Psi_0 | \hat{H}_v | \Psi_0 \rangle = E_0$ and $\langle {\Psi_0}' | \hat{H}_{v'} | {\Psi_0}' \rangle = E'_0$ leads to

$$E_0 + \langle \Psi_0 | v'_{ext} - v_{ext} | \Psi_0 \rangle + {E_0}' + \langle {\Psi_0}' | v_{ext} - v'_{ext} | {\Psi_0}' \rangle > {E_0}' + E_0 \tag{6}$$

By inserting (3) and (4), which are valid because of the assumption that the two different ground-state wavefunctions Ψ_0 and Ψ'_0 lead to the same ground-state density $n_0(\underline{r})$, one obtains $E_0 + {E_0}' > {E_0}' + E_0$, which is clearly a contradiction, and the assumption cannot be true. Consequently, two external potentials $v_{ext} \neq v'_{ext} + const$ cannot lead to the same ground-state density. Therefore, the ground-state density uniquely determines the external potential up to a trivial constant and thus via the many-electron Schrödinger equation uniquely the many-electron wavefunctions of the system. This means that all stationary observables of the many-electron system are uniquely determined by the ground-state density. Unfortunately, for most physical properties it is not known how they can be calculated directly from the ground-state density without using the many-electron Schrödinger equation so that the unique determination is not often of practical use.

To calculate the ground-state energy E_0 the unique energy functional $E[n(\underline{r})]$ can be defined[10] by

$$E[n(\underline{r})] = \min_{\Psi \to n(\underline{r})} \langle \Psi | \hat{T} + \hat{U} + v_{ext} | \Psi \rangle = F[n(\underline{r})] + \int n(\underline{r}) v_{ext}(\underline{r}) \mathrm{d}\underline{r} \,, \tag{7}$$

where the minimum is over all wavefunctions, which give the density $n(\underline{r})$. The functional

$$F[n(\underline{r})] = \min_{\Psi \to n(\underline{r})} \langle \Psi | \hat{T} + \hat{U} | \Psi \rangle \tag{8}$$

does not depend on the external potential v_{ext} and but only on $\hat{T}$ and $\hat{U}$ and is universal in the sense that it is same for all systems described by the Schrödinger equation (1). From (7) one obtains the inequality

$$E[n(\underline{r})] \leq \langle \Psi | \hat{T} + \hat{U} + v_{ext} | \Psi \rangle \tag{9}$$

for all wavefunctions Ψ, which give the density $n(\underline{r})$. For the ground-state wavefunction Ψ_0 with the ground-state density $n_0(\underline{r})$ this means $E[n_0(\underline{r})] \leq \langle \Psi_0 | \hat{T} + \hat{U} + v_{ext} | \Psi_0 \rangle = E_0$. Since $\langle \Psi | \hat{T} + \hat{U} + v_{ext} | \Psi \rangle \geq E_0$ is valid for all wavefunctions because of the Rayleigh-Ritz minimum principle, this inequality is also valid for the wavefunction which leads to the minimum in (7). This means $E[n(\underline{r})] \geq E_0$ is valid for all densities, in particular for the ground-state density: $E[n_0(\underline{r})] \geq E_0$. Together with $E[n_0(\underline{r})] \leq E_0$ this shows $E_0 = E[n_0(\underline{r})]$ which proves the second part of the Hohenberg-Kohn theorem: the minimum of $E[n(\underline{r})]$ is obtained for the ground-state density and this minimum gives the ground-state energy

$$E_0 = \min_n E[n(\underline{r})] \,. \tag{10}$$

Here the minimization is over all densities which arise from antisymmetric wavefunctions for N electrons.

2.2 Kohn-Sham Equations

The theory discussed above has transformed the problem of finding the minimum of $\langle \Psi | \hat{H} | \Psi \rangle$ for many-electron trial wavefunctions Ψ into the seemingly much more simple problem of finding the minimum of $E[n(\underline{r})]$ for trial densities $n(\underline{r})$ which depend on only three space variables. However, since the explicit form of the functional $F[n(\underline{r})]$ is not known, the theory is rather abstract. Here, the idea of Kohn and Sham[9], the introduction of a fictitious auxiliary non-interacting electron system with the same ground-state density is of extraordinary importance. Because the Hohenberg-Kohn theorem is valid for all interaction strengths (that is for all values of e^2), it is also valid for the choice $e^2 = 0$ which according to (1) describes a non-interacting system with $U(\underline{r}, \underline{r}') = 0$. By the Hohenberg-Kohn theorem the ground-state density uniquely determines the external potential in the non-interacting system. This potential is usually called the effective potential $v_{eff}(\underline{r})$. For the non-interacting system the total energy functional (7) can be written as

$$E[n(\underline{r})] = T_s[n(\underline{r})] + \int n(\underline{r}) v_{eff}(\underline{r}) \mathrm{d}\underline{r} \tag{11}$$

because the functional $F[n(\underline{r})]$ (for $e^2 = 0$) reduces to the kinetic energy functional $T_s[n(\underline{r})]$ of non-interacting electrons. For the non-interacting system with potential

$v_{eff}(\underline{r})$ the ground-state density $n_0(\underline{r})$ and the ground-state kinetic energy $T_s[n_0(\underline{r})]$ can be calculated exactly by

$$n_0(\underline{r}) = \sum_i |\varphi_i(\underline{r})|^2 \quad \text{and} \quad T_s[n_0(\underline{r})] = \sum_i \int \varphi_i^\star(\underline{r})(-\frac{\hbar^2}{2m}\nabla_{\underline{r}}^2)\varphi_i(\underline{r})\mathrm{d}\underline{r}\,, \tag{12}$$

where $\varphi_i(\underline{r})$ are the Kohn-Sham wavefunctions (orbitals), which are obtained by solving a single-particle Schrödinger equation

$$\hat{H}_s\varphi_i(\underline{r}) = \left[-\frac{\hbar^2}{2m}\nabla_{\underline{r}}^2 + v_{eff}(\underline{r})\right]\varphi_i(\underline{r}) = \epsilon_i\varphi_i(\underline{r})\,. \tag{13}$$

The sums in (12) are over the N wavefunctions with lowest values of ϵ_i. To apply this scheme, a useful expression for the effective potential $v_{eff}(\underline{r})$ must be found. The important achievement of Kohn and Sham was the suggestion to separate the unknown functional $F[n(\underline{r})]$ in (7) into a sum of known terms and into an unknown, hopefully much smaller rest which must be approximated. The energy functional is written as

$$E[n(\underline{r})] = T_s[n(\underline{r})] + \int n(\underline{r})v_{ext}(\underline{r})\mathrm{d}\underline{r} + \frac{e^2}{2}\iint \frac{n(\underline{r})n(\underline{r}')}{|\underline{r}-\underline{r}'|}\mathrm{d}\underline{r}\mathrm{d}\underline{r}' + E_{xc}[n(\underline{r})]\,, \tag{14}$$

where the term which contains density products describes the classical electron-electron interaction (Hartree interaction) and the last term is the exchange-correlation energy functional defined as

$$E_{xc}[n(\underline{r})] = F[n(\underline{r})] - T_s[n(\underline{r})] - \frac{e^2}{2}\iint \frac{n(\underline{r})n(\underline{r}')}{|\underline{r}-\underline{r}'|}\mathrm{d}\underline{r}\mathrm{d}\underline{r}'\,. \tag{15}$$

For the ground-state density comparison of (11) and (14) shows that

$$\int n(\underline{r})v_{eff}(\underline{r})\mathrm{d}\underline{r} = \int n(\underline{r})v_{ext}(\underline{r})\mathrm{d}\underline{r} + \frac{e^2}{2}\iint \frac{n(\underline{r})n(\underline{r}')}{|\underline{r}-\underline{r}'|}\mathrm{d}\underline{r}\mathrm{d}\underline{r}' + E_{xc}[n(\underline{r})]\,. \tag{16}$$

is valid except for an unimportant trivial constant. The functional derivative of (16) with respect to $n(\underline{r})$ is given by

$$v_{eff}(\underline{r}) = v_{ext}(\underline{r}) + e^2\int \frac{n(\underline{r}')}{|\underline{r}-\underline{r}'|}\mathrm{d}\underline{r}' \; + v_{xc}[n(\underline{r})](\underline{r})\,, \tag{17}$$

where the exchange-correlation potential

$$v_{xc}[n(\underline{r})](\underline{r}) = \frac{\delta E_{xc}[n(\underline{r})]}{\delta n(\underline{r})} \tag{18}$$

is defined for every point $\underline{r}$ as a functional of the density. Equations (12) and (13) are technically single-particle equations with a local effective potential $v_{eff}(\underline{r})$. This local potential makes density functional calculations simpler than Hartree-Fock calculations where the potential is non-local acting as $\int V_{HF}(\underline{r},\underline{r}')\varphi_i(\underline{r}')\mathrm{d}\underline{r}'$.

The effective potential (17) depends on the density, which in turn depends on the effective potential according to (12) and (13). These equations must be solved self-consistently, which can be achieved by iteration: starting with a reasonable trial density the effective potential is calculated by (17). Then (12) and (13) are solved to determine a new density which is used again in (17). This process is repeated until input and output density of an iteration agree within the required accuracy. The straightforward iteration usually leads

to oscillations with increasing amplitude. The oscillation can be damped by input-output mixing or by more sophisticated schemes[11]. From the behaviour of the eigenvalues of the functional derivative $f(\underline{r}, \underline{r}') = \delta E[n(\underline{r})]/\delta n(\underline{r}')$ it can be concluded[12] that the mixing process always converges to a stable solution if small enough mixing parameters are used, but many iterations may be needed.

The single-particle states φ_i and the single-particle energies ϵ_i obtained by solving (13) are properties of the *non-interacting auxiliary* system. In the interacting system they have no physical meaning and their interpretation as measurable quantities is not justified, although this interpretation is often adequate. A particular problem connected with the energies ϵ_i is that the eigenvalue gap between unoccupied and unoccupied states can differ considerably from the fundamental physical gap Δ in insulators and semiconductors. This gap is defined as $\Delta = [E(N+1) - E(N)] - [E(N) - E(N-1)]$ as the difference of the energies required for adding and removing one electron. Here $E(N)$, $E(N+1)$ and $E(N-1)$ are the ground-state total energies of the system with N, $N+1$ and $N-1$ electrons.

2.3 Approximations for the Exchange-Correlation Energy Functional

In principle, density functional theory is exact, but since all complications of the many-particle problem are hidden in the functional $E_{xc}[n(\underline{r})]$, which is not known explicitly, the success of density functional calculations depends on whether reasonable approximations for this functional can be found. A rather simple and remarkably good approximation is the replacement of the exact functional E_{xc} by

$$E_{xc}^{LDA}[n(\underline{r})] = \int n(\underline{r})\, \epsilon_{xc}^{LDA}(n(\underline{r}))\, \mathrm{d}\underline{r}\,, \tag{19}$$

the so-called local density approximation (LDA), where $\epsilon_{xc}^{LDA}(n)$ is a function (not a functional) of the density. For a homogeneous interacting electron system with constant density, the local density approximation is exact and $\epsilon_{xc}^{LDA}(n)$ can be determined as function of n by quantum mechanical many-body calculations. The exchange part $\epsilon_x^{LDA}(n)$ of $\epsilon_{xc}^{LDA}(n)$ is simple and given by

$$\epsilon_x^{LDA}(n) = -\frac{3e^2}{4}\left(\frac{3}{\pi}\right)^{1/3} n^{1/3}\,, \tag{20}$$

whereas the correlation part $\epsilon_c^{LDA}(n)$ is more difficult to calculate. Accurate results for $\epsilon_c^{LDA}(n)$ have been obtained by the quantum Monte Carlo method[13] and reliable parametrizations[14,15] for these results are available.

For systems with more inhomogeneous densities, the integrand in (19) can be generalized by using the gradient $\nabla n(\underline{r})$ of the density, for instance in the form,

$$E_{xc}^{GGA}[n(\underline{r})] = \int f(n(\underline{r}), \nabla n(\underline{r}))\, \mathrm{d}\underline{r}\,. \tag{21}$$

While the input ϵ_{xc}^{LDA} in (19) is unique, the function f in (21) is not and different forms have been suggested incorporating a number of known properties of the exact functional, for instance scaling and limit behaviours, or empirical parameters. A well tested numerical approximation is the generalized gradient approximation (GGA)[16–18], which for instance,

improves the cohesive energies and lattice constants of the 3d transition metals. So-called meta-GGA functionals[19,20] were also proposed, where besides the local density and its gradient also other variables are introduced, for instance the kinetic energy density of the Kohn-Sham orbitals

$$E_{xc}^{meta-GGA}[n(\underline{r})] = \int f\left(n(\underline{r}), \nabla n(\underline{r}), \tau(\underline{r})\right) \mathrm{d}\underline{r} \quad \text{with} \quad \tau(\underline{r}) = \sum_i |\nabla \varphi_i(\underline{r})|^2 . \tag{22}$$

By the additional flexibility in (22) it has been possible to improve the accuracy compared to (21) for some physical properties without worsening the results for others.

Probably the most serious shortcoming of the exchange-correlation functionals presented above is that they do not provide a cancellation of the self-interaction arising from the classical Hartree term which is used in (14). This shortcoming is particularly problematic in systems with localized and strongly interacting electrons as transition metal oxides and rare earth elements and compounds. Several techniques have been suggested to deal with self-interaction problem. Perdew and Zunger[15] suggested to use a self-interaction corrected (SIC) functional, where the self-interaction is removed explicitly for each orbital. In the LDA+U method[21] explicit on-site Coulomb interaction terms are added. Another way to treat the problem is to use the so-called exact exchange expression

$$E_x^{KS}[n(\underline{r})] = -\sum_{ij} \iint \frac{\varphi_i^\star(\underline{r}')\varphi_i(\underline{r})\varphi_j^\star(\underline{r})\varphi_j(\underline{r}')}{|\underline{r} - \underline{r}'|} \mathrm{d}\underline{r}\mathrm{d}\underline{r}' \tag{23}$$

as part of energy functional. Note that $E_x^{KS}[n(\underline{r})]$ as well as $T_s[n(\underline{r})]$ given in (12) and $\tau(\underline{r})$ given in (22) are defined by the Kohn-Sham orbitals $\varphi_i(\underline{r})$. Nevertheless, they are still density functionals, since by (13) the orbitals are determined by the effective potential and thus by the density because of the Hohenberg-Kohn theorem. One problem[22] with the use of exact exchange is to treat correlation in a way which is compatible with the exchange (23). In chemistry hybrid functionals, for instance

$$E_{xc}^{hyb} = aE_x^{KS} + (1-a)E_x^{GGA} + E_c^{GGA} \tag{24}$$

as suggested by Becke[23,24], are rather popular, where the constant $a \approx 0.28$ is an empirical parameter. Another, even more popular example is the B3LYP (Becke[24], three-parameter, Lee-Yang-Parr[25]) exchange-correlation functional

$$E_{xc}^{B3LYP} = E_{xc}^{LDA} + a_0(E_x^{KS} - E_x^{LDA}) + a_x(E_x^{GGA} - E_x^{LDA}) + a_c(E_c^{GGA} - E_c^{LDA}) \tag{25}$$

which combines the exchange E_x^{KS} with exchange and correlation functionals of LDA and GGA type with three empirically fitted parameters. Technically, self-consistent calculations with E_x^{KS} are rather involved because the exchange potential v_x^{KS} defined as the functional derivative of $E_x^{KS}[n(\underline{r})]$ with respect to $n(\underline{r})$ is difficult to calculate[22].

2.4 Solution methods

Although in density functional theory only single-particle equations with a local potential must be solved, the required computations can be a challenging task, in particular for complex and large systems. Thus it cannot be considered as a surprise that the Nobel Prize in Chemistry 1998 was not only awarded to Walter Kohn “for his development of

the density functional theory", but also to John A. Pople "for his development of computational methods in quantum chemistry". Standard solution methods for the Kohn-Sham equation (13) usually apply an expansion of the single-particle wavefunctions in a set of basis functions and use the Rayleigh-Ritz variational principle to determine the expansion coefficients.

Historically, solution methods can be classified into three categories using plane waves, localized atomic(-like) orbitals or the atomic sphere concept. Plane waves are simple and a natural basis for periodic systems, but inadequate to represent the large variations of the low lying atomic core states so that plane waves usually require to replace the strong potential near the nuclei by a much weaker pseudopotential. Localized orbitals, for instance Gaussian, Slater or numerically constructed orbitals, are well suited to describe atomic-like features in molecules and solids and are widely used, in particular in chemistry. In atomic sphere methods different representations for the wavefunctions are used in the spheres around the atomic centers, where the wavefunctions rapidly vary particularly near the nuclei, and in the interstitial region between the spheres, where the wavefunctions behave smoothly. In the original atomic sphere methods, in Slater's augmented plane wave (APW) method and in the Korringa-Kohn-Rostoker (KKR) method this separation resulted in a complicated non-linear energy dependence. Here Andersen's development[26] of the linear augmented plane wave (LAPW) and the linear muffin-tin orbital (LMTO) method by linearizing the energy dependence was a real breakthrough for the use of atomic sphere methods.

A disadvantage of basis set methods is that, although the basis set (chosen by physical motivation) often yields acceptable results for a small number of basis functions, precise calculations can be rather costly because they may require a large number of basis functions. Due to these limitations, in recent years purely numerical methods have been developed to solve the Kohn-Sham (Schrödinger) equation, for instance by using finite differences,[27] finite elements,[28] multigrid[28–30] or wavelet[31,32] methods.

3 Linear Scaling

Although over the last decades the computational efficiency to solve the density functional equations has increased significantly, the system size which can be studied is still rather limited. Systems with a few hundred atoms can be treated routinely today, but larger systems with thousands of atoms require enormous computer resources, if standard techniques are used to solve the density functional equations. The main bottleneck is that the computing time in standard calculations increases with the third power of the number of atoms (electrons) in the system. Although the computing power has increased by a factor of ten every four years (Moore's law) in the past and one can expect a similar increase in the next years, one has to wait for more than a decade until a ten times larger system can be treated if standard density functional methods with their $O(N^3)$ behaviour of the computing time are used.

Since about ten years considerable effort has been spent to remove the $O(N^3)$ bottleneck in most or all parts of the computer codes for density functional calculations. Most of this work is based on a locality principle, the nearsightedness of electronic matter, which has been formulated in a series of papers by Kohn[33,34]. Another possibility is to exploit the inherent $O(N)$ capability of multigrid[35] and multiresolution[36] (wavelet) methods.

The nearsightedness principle means that in systems without long range electric fields (and for fixed chemical potential) the density change at a point r_0, which is caused by a potential change in a finite region far away (outside a sphere with radius R around r_0), is small and decays to zero if R increases to infinity. Thus the charge density in a region (for instance in the central region shown in Fig. 1) can be calculated from the potential in this region and from the potential in a surrounding buffer region, whereas the potential outside the buffer region can be neglected. This concept is directly exploited in divide and conquer techniques (see below).

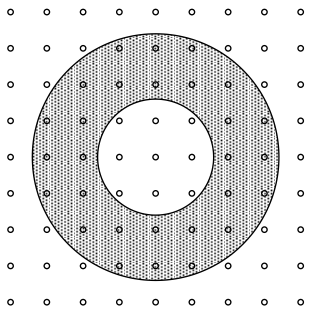

Figure 1. Schematic view of the central and the surrounding buffer region (in gray). The atomic positions are denoted by small circles.

A possibility to avoid the calculation of eigenstates which extend over the entire system is to work with the density matrix. For non-interacting particles the density matrix can be written in terms of the Kohn-Sham orbitals φ_i (the eigenstates of the non-interacting auxiliary system) for zero temperature as

$$\rho(\underline{r},\underline{r}') = \sum_i \varphi_i^\star(\underline{r})\varphi_i(\underline{r}') \tag{26}$$

and for non-zero temperature as

$$\rho(\underline{r},\underline{r}') = \sum_i f_i\varphi_i^\star(\underline{r})\varphi_i(\underline{r}') \;, \tag{27}$$

where the occupation numbers are given by $f_i = f((\epsilon_i - E_F)/kT)$. For $T = 0$ the sum is restricted to the occupied eigenstates, whereas for $T \neq 0$ all eigenstates are used. However, due to the decay of the Fermi-Dirac function $f(x) = (1 + \exp(x))^{-1}$ only low lying unoccupied states give appreciable contributions. In terms of the density matrix the density and kinetic energy given in (12) can be written as

$$n(\underline{r}) = \rho(\underline{r},\underline{r}) \quad \text{and} \quad T_s[n(\underline{r})] = \int \lim_{\underline{r}\to\underline{r}'} \left[-\frac{\hbar^2}{2m}\nabla^2_{\underline{r}}\rho(\underline{r},\underline{r}')\right] \mathrm{d}\underline{r}' \tag{28}$$

which shows that the effective potential (17) and all parts of the energy functional (14) can be calculated if $\rho(\underline{r},\underline{r}')$ is known. According to the nearsightedness principle the density matrix decays to zero for $|\underline{r} - \underline{r}'| \to \infty$. In insulators and semiconductors the decay is exponential for large distance[37–39]

$$\rho(\underline{r},\underline{r}') \sim \exp(-\gamma|\underline{r} - \underline{r}'|) \;, \tag{29}$$

whereas in metallic systems (at zero temperature) the decays is only algebraical

$$\rho(\underline{r},\underline{r}') \sim \frac{\cos(k_F|\underline{r}-\underline{r}'|)}{|\underline{r}-\underline{r}'|^2}\,, \tag{30}$$

where γ increases with the size of the band gap and $k_F = \sqrt{2mE_F}/\hbar$ denotes the Fermi wavevector.

3.1 Divide and Conquer Technique

A straightforward way to exploit the nearsightedness principle is to divide the system into overlapping subsystems and to solve the Kohn-Sham equations separately in each subsystem by standard methods taking into account an atom or a group of atoms in a central region surrounded by a buffer region. The density of the central regions is used and the density of the buffer regions is neglected. Examples of this approach are the divide and conquer technique proposed Yang[40] and the locally self-consistent multiple-scattering[41] (LSMS) or locally self-consistent Green function[42,43] (LSGF) methods which are based on KKR or LMTO calculations. Since each local interaction zone consisting of the central and its surrounding buffer region is treated independently, the effort in this approach scales linearly with system size and is parallelized easily over atoms or groups of atoms. A disadvantage is the limited accuracy[44] which can be achieved with a computationally affordable number of atoms in the local interaction zone since the effort increases cubically with this number.

3.2 Fermi Operator Expansion

The Kohn-Sham orbitals in (27) are eigenfunctions of the Hamilton operator $\hat{H}_s$ according to (13). From $\hat{H}_s\varphi_i = \epsilon_i\varphi_i$ one obtains $f((\hat{H}_s - E_F)/kT)\varphi_i = f_i\varphi_i$ and (27) can be written as

$$\rho(\underline{r},\underline{r}') = F(\hat{H}_s)\sum_i \varphi_i^\star(\underline{r})\varphi_i(\underline{r}') \tag{31}$$

with $F(\hat{H}_s) = f((\hat{H}_s - E_F)/kT)$. Since the sum in (31) is over all orbitals an arbitrary unitary transformation $\phi_i = \sum_j U_{ij}\varphi_j$ with $\sum_i U_{ik}^\star U_{ij} = \delta_{kj}$ can be used to rewrite (31) as

$$\rho(\underline{r},\underline{r}') = F(\hat{H}_s)\sum_i \phi_i^\star(\underline{r})\phi_i(\underline{r}') \tag{32}$$

This means that any complete set of basis functions can be used to evaluate the density matrix without the need to calculate explicitly the Kohn-Sham wavefunctions provided that one knows how to calculate $F(\hat{H}_s)\phi_i(\underline{r}')$. In the Fermi operator method[39,45] the Fermi function is expanded into Chebyshev polynomials so that $F(\hat{H}_s)$ is a polynomial in $\hat{H}_s$. Its action on the basis function $\phi_i(\underline{r}')$ is calculated according to the recursion relations of the Chebyshev polynomials by subsequent applications of $\hat{H}_s$. Linear scaling is obtained by neglecting the small elements of $F(\hat{H}_s)\phi_i(\underline{r}')$ which appear due to the exponential decay of the density matrix. Note that the use of Chebyshev polynomials requires that the eigenvalues of the Hamilton operator are in the interval $[-1,1]$ which can be achieved by shifting

and scaling. Similar in spirit to the Fermi operator expansion, which for $T \to 0$ corresponds to a polynomial expansion of a step function, is the kernel polynomial method[46] which uses a polynomial expansion of the δ function with factors designed to reduce the Gibbs oscillations arising from polynomial expansions of step or delta functions.

3.3 Recursion Method

The recursive application of a Hamilton operator to a basis set is also the essence of the recursion method[47,48] which is based on the Lanczos algorithm. The recursion method gives a continued fraction expansion for the density of states and for diagonal elements of the resolvent $E - \hat{H}_s$. It is used together with with divide and conquer approach, for instance, in the OpenMX program[49] based on a Krylov-subspace method[50,51].

3.4 Density Matrix Minimization

In the density matrix minimization approach[52–54] a direct minimization of the total energy with respect to the density matrix is performed. Here two constraints must be satisfied. The trial density matrix must give the correct number of electrons, $N = \int n(\underline{r})\mathrm{d}\underline{r} = \int \rho(\underline{r},\underline{r})\mathrm{d}\underline{r}$, and it must be idempotent $\hat{\rho}^2 = \hat{\rho}$ which means that

$$\int \rho(\underline{r},\underline{r}'')\rho(\underline{r}'',\underline{r}')\mathrm{d}\underline{r}'' = \rho(\underline{r},\underline{r}') \tag{33}$$

must be satisfied. This equation is equivalent to the requirement that all eigenvalues of the density matrix operator $\hat{\rho}$ are equal to one or zero. The constraint $N = \int \rho(\underline{r},\underline{r})\mathrm{d}\underline{r}$ can be treated by a Lagrange parameter which amounts to replacing the minimization of the total energy by minimization of the grand potential. The constraint of idempotency is taken into account by the "McWeeny purification"[55] which means to express $\hat{\rho}$ by $\hat{\rho} = 3\hat{\sigma}^2 - 2\hat{\sigma}^3$ with an auxiliary trial density matrix operator $\hat{\sigma}$. Provided that the trial operator $\hat{\sigma}$ has eigenvalues between -1/2 and 3/2, the eigenvalues of $\hat{\rho}$ are between 0 and 1 and the minimization process becomes a stable algorithm which drives the density matrix towards idempotency[52]. In the last years programs as CONQUEST[56] and ONETEP[57] have appeared which achieve linear-scaling by utilizing the decay of the density matrix[58–60].

3.5 Local Orbital Method

In the local orbital method[61–63] the Kohn-Sham energy functional is generalized by replacing (12) with

$$n(\underline{r}) = \sum_{ij} A_{ij}\phi_i^\star(\underline{r})\phi_j(\underline{r}) \quad \text{and} \quad T_s[n(\underline{r})] = \sum_{ij} A_{ij}\int \phi_i^\star(\underline{r})(-\frac{\hbar^2}{2m}\nabla_{\underline{r}}^2)\phi_j(\underline{r})\mathrm{d}\underline{r}\,, \tag{34}$$

where ϕ_i are non-orthogonal local orbitals. For $A_{ij} = \delta_{ij}$ this generalized functional agrees with the original Kohn-Sham functional and for $A_{ij} = S_{ij}^{-1}$, where $S_{ij} = \langle\phi_i|\phi_j\rangle$ is the overlap matrix, one obtains the correct functional for non-orthogonal orbitals. The problem with the choice $A = S^{-1}$ is that, whereas the overlap matrix is sparse for local

orbitals, its inverse is not sparse. To avoid the calculation of S^{-1} the local orbital method uses[61,63]

$$A = \sum_{k=0}^{n} (1 - S)^k \tag{35}$$

or the special choice[62] $n = 1$ which leads to $A = 2 - S$. During minimization the generalized functional approaches the correct one, but orthogonalization or calculation of the inverse of the overlap matrix, both requiring $O(N^3)$ operations, are avoided. Linear scaling with in the local orbital method is achieved by utilizing the decay of the density matrix[64], for instance within the SIESTA[65] program.

4 A Linear Scaling Algorithm for Metallic Systems

Since the density matrix decay in metals is only algebraical, an obvious idea is to make the decay faster by using a non-zero temperature. For $T \neq 0$ the density matrix in metals behaves for large distance as[36,37]

$$\rho(\underline{r}, \underline{r}', T) \sim \frac{\cos(k_F|\underline{r} - \underline{r}'|)}{|\underline{r} - \underline{r}'|^2} \exp(-\gamma|\underline{r} - \underline{r}'|) \,, \tag{36}$$

but it is not clear whether the decay constant γ, which is proportional to temperature, is large enough for reasonable temperatures so that linear scaling techniques developed for insulating systems can be applied also for metallic systems. Another difficulty for density matrix based techniques is that in metals no gap exists between occupied and unoccupied states so that an unambiguous choice of the states contributing to the density matrix is nontrivial. Nevertheless, some success has already been achieved for metallic systems[51,60].

Recently a linear scaling algorithm suitable for metals has been proposed in our institute[66,67]. This algorithm is based on the tight-binding (TB) version of the KKR Green function method[68,69] and on the electronic nearsightedness by exploiting a relation between finite-temperature density matrix and Green function. The principle of nearsightedness has been applied in KKR and LMTO calculations already for years, for instance for the embedding of impurities[70–72], where the fact is used that local potential perturbations lead to negligible density changes at large distance, and in the LSMS and LSGF methods discussed above. Compared to the LSMS and LSGF methods our algorithm seems to be more advantageous since in addition to the nearsightedness principle it also exploits the sparsity of the TB-KKR matrix. This sparsity alone leads already to an $O(N^2)$ behaviour of the computing time if the KKR matrix equations are solved by iteration.

4.1 Basic KKR Green Function Equations

Compared to wavefunction methods, where the density is calculated according to (12), the KKR Green function method obtains the density by

$$n(\underline{r}) = -\frac{2}{\pi} \mathrm{Im} \int_{-\infty}^{E_F} G(\underline{r}, \underline{r}; E) \mathrm{d}E \tag{37}$$

as an energy integral over the independent-particle Kohn-Sham Green function $G(\underline{r},\underline{r};E)$ which is defined as the solution of

$$\left[-\frac{\hbar^2}{2m}\nabla^2_{\underline{r}}+v_{eff}(\underline{r})-E\right]G(\underline{r},\underline{r}';E)=-\delta(\underline{r}-\underline{r}') \tag{38}$$

with the boundary condition $G(\underline{r},\underline{r}';E)\rightarrow 0$ for $|\underline{r}-\underline{r}'|\rightarrow\infty$. For the calculation of $G(\underline{r},\underline{r}';E)$ it is convenient to transform the differential equation (38) into an equivalent integral equation[69]

$$G(\underline{r},\underline{r}';E)=G^r(\underline{r},\underline{r}';E)+\int G^r(\underline{r},\underline{r}'';E)\left[v_{eff}(\underline{r}'')-v^r(\underline{r}'')\right]G(\underline{r}'',\underline{r}';E)\mathrm{d}\underline{r}'', \tag{39}$$

where v^r is the potential of a reference system, for which the Green function G^r is assumed to be known. This integral over all space is then divided into integrals over non-overlapping space-filling cells around the atomic positions $\underline{R}^n$. In each cell the multiple-scattering representation[69]

$$G(\underline{r}+\underline{R}^n,\underline{r}'+\underline{R}^{n'};E)=\delta^{nn'}G^n_s(\underline{r},\underline{r}';E)+\sum_{LL'}R^n_L(\underline{r};E)G^{nn'}_{LL'}(E)R^{n'}_{L'}(\underline{r}';E) \tag{40}$$

of the Green function is used, where L stands for the angular-momentum indices l and m and $\underline{r}$ and $\underline{r}'$ are cell-centred coordinates. With this representation the integral equation (39) can be solved by a matrix equation[69,73]

$$G^{nn'}_{LL'}(E)=G^{r,nn'}_{LL'}(E)+\sum_{n''L''L'''}G^{r,nn''}_{LL''}(E)\Delta t^{n''}_{L''L'''}(E)G^{n''n'}_{L'''L'}(E)\,. \tag{41}$$

Here the matrices have the dimension $N_{at}(l_{max}+1)^2$, where N_{at} is the number of atoms and l_{max} is the highest angular momentum l used (usually $l_{max}=3$ is sufficient). In (41) the Green function matrix elements $G^{nn'}_{LL'}(E)$ are the ones of the system and $G^{r,nn'}_{LL'}(E)$ are the ones of the reference system. These matrix elements are the only quantities in the KKR Green-function method which couple different atomic cells, whereas the single-scattering Green functions $G^n_s(\underline{r},\underline{r}';E)$ and wavefunctions $R^n_L(\underline{r};E)$ depend only on the potential $v_{eff}(\underline{r})$ inside cell n and the single-scattering t-matrix differences $\Delta t^n_{LL'}(E)$ only on the difference $v_{eff}(\underline{r})-v^r(\underline{r})$ of the potential and the reference potential inside cell n. All these single-scattering quantities can be calculated independently for each cell as described in[69,74] with a computational effort which naturally scales with the number of atoms. This means that for large systems the solution of (41) with its $O(N^3)$ computing effort requires by far the largest part of the computer resources, if the standard KKR Green function method is used, where due to free space as reference system the matrices in (41) are dense matrices.

Here the question is whether a reference system can be found, where the Green function matrix $G^{r,nn'}_{LL'}(E)$ is sparse, and whether the matrix equation (41) can be solved by iterative methods. This would reduce the computing effort from $O(N^3)$ to $O(N^2)$. Actually, only $O(N)$ elements of $G^{nn'}_{LL'}(E)$ with $n=n'$ are used for the density calculation, but in three-dimensional space the calculation of the $n=n'$ elements without the knowledge all other elements $G^{nn'}_{LL'}(E)$ seems to be impossible. In one-dimensional situations (e. g. for layered systems with two-dimensional periodicity) linear scaling algorithms to obtain the diagonal ($n=n'$) elements are known. Note that in one dimension the sparsity pattern of the Green

function matrix corresponds to a banded matrix with a bandwidth independent of the size of the system.

4.2 Repulsive Reference System

The standard reference system in the KKR method is free space. Here the Green function matrix elements $G_{LL'}^{0,nn'}(E)$ are analytically known, but decay rather slowly with distance between site n and n'. A reference system with exponentially decaying matrix elements can be obtained by using a repulsive potential. A useful reference system[68], where the matrix elements $G_{LL'}^{r,nn'}(E)$ can be calculated with moderate effort and without spoiling the rapid angular momentum convergence ($l \leq l_{max} = 3$), consists of an infinite array of repulsive potentials confined to nonoverlapping muffin-tin spheres around the sites $\underline{R}^n$ as it is schematically shown in Fig. 2. The matrix elements of this reference system, also called screened structure constants, can be calculated in real space by solving

$$G_{LL'}^{r,nn'}(E) = G_{LL'}^{0,nn'}(E) + \sum_{n''L''L'''} G_{LL''}^{0,nn''}(E) t_{L''L'''}^{r,n''}(E) G_{L'''L'}^{r,n''n'}(E) \qquad (42)$$

with reference t matrices $t_{L''L'''}^{r,n''}(E)$ which for each cell n'' are determined by the repulsive reference potential in this cell. Due to the rapid decay of $G_{L'''L'}^{r,n''n'}(E)$ with distance $|\underline{R}^{n''} - \underline{R}^{n'}|$, only a finite number N_{cl} of sites n'' contribute appreciably to the sum over n'' in (42). The neglect of more distant sites in (42) leads to a matrix equation of dimension $N_{cl}(l_{max}+1)^2$ which for each site n' can be solved independently. Setting exponentially small elements of $G_{LL''}^{r,nn''}(E)$ to zero makes this matrix sparse with a sparsity degree N_{cl}/N_{at} and reduces the computational effort to solve (41). The effort is then proportional to $N_{it}N_{cl}N_{at}^2$ instead of N_{at}^3 provided that (41) can be solved iteratively in N_{it} iterations.

4.3 Complex Energy Integration

One difficulty for the iterative solution of (41) is that iterations cannot converge at or near energies E, where the Green function $G(\underline{r}, \underline{r}'; E)$ has singularities. Such singularities appear on the real energy axis as poles (bound states) resembling the atomic core states and branch cuts (continuous eigenstates) resembling the valence and conduction bands. The difficulty is avoided if complex energies E with $\mathrm{Im}E \neq 0$ are used, which is straightforward in the KKR Green function method since the equations (38–42) are also valid for complex E. Moreover, since the Green function is an analytic function of E for $\mathrm{Im}E \neq 0$, the density (37) can be calculated by contour integration in the complex energy plane[75]. The necessarily real energy E_F at the end point of the contour is avoided by using the finite-temperature density functional formalism[76], where (37) is replaced by[69,77]

$$n(\underline{r}) = -\frac{2}{\pi}\mathrm{Im}\int_{-\infty}^{\infty} f(E - E_F, T) G(\underline{r}, \underline{r}; E)\mathrm{d}E\,. \qquad (43)$$

This integral can be calculated by a contour as shown in Fig. 2, where a typical set of integration mesh points is represented by crosses. The mesh points vertically above E_F correspond to singularities of the Fermi function (the so-called Matsubara energies) $E_j = E_F + (2j-1)\mathrm{i}\pi kT$ with $j = 1, 2, ...$ The other points are Gaussian integration points

constructed as described in Ref. 67. The contour starts on the negative real energy axis in the energy gap above the core and below the valence states. From there the contour goes parallel to the imaginary axis up to a chosen distance and then to infinity parallel to the real axis. The distance from the real axis is chosen as $2J\pi kT$, where J denotes the number of Matsubara energies at which the residues must be taken into account. Note that on the part of the contour, which is parallel to the real axis, the Fermi function is real as on the real axis due to its periodicity with period $2\mathrm{i}\pi kT$ and that practically no point with $\mathrm{Re}E > E_F$ exists because of the rapid decay of $f(E - E_F, T)$ for $\mathrm{Re}E > E_F$. The thick line in Fig. 2 along the real axis denotes the original integration of path of (37). The contour integration includes only contributions of valence states and the contributions of core states must be added separately.

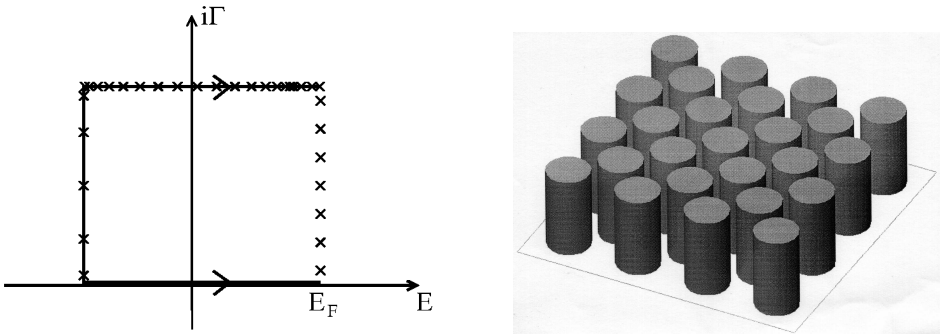

Figure 2. Integration contour in the complex energy plane with mesh points indicated by crosses (left picture) and a schematic view (in two dimensions) of a repulsive reference system with muffin-tin potentials of constant height (right picture).

4.4 Iterative Solution

Another difficulty for the iterative solution of (41) is that straightforward iteration, for instance in the form

$$G_{i+1}(E) = G^r(E) + G^r(E)\Delta t(E)G_i(E)\,, \tag{44}$$

which corresponds to the Born iterations in scattering theory, usually diverges. We found that convergent iterations can be obtained by Anderson mixing[11,78], which is used also sometimes to accelerate the density functional self-consistency. Anderson mixing combines input and output information of all previous iterations to prepare an optimal input for the next iteration. A disadvantage of Anderson mixing is that all this information must be kept which leads to large storage requirements. Alternatively, (41) can be solved iteratively by use of standard techniques which have been developed for systems of linear equations. With the TB-KKR matrix $M(E) = 1 - G^r(E)\Delta t(E)$, which for complex E is a complex non-Hermitian matrix, equation (41) can be written as a system of linear equations $M(E)G(E) = G^r(E)$. We found that the quasi-minimal-residual (QMR) method[79,80] in

its transpose free version is suitable to solve (41). The QMR method requires to store information from a few iterations and was better suited for the large supercells considered below than Anderson mixing.

An important feature of iterative solution is that each atom n' and each angular momentum component L' in (41) can be treated independently so that iterative solution is ideally suited for massively parallel computing. The independent treatment of each atom is in the spirit of the divide and conquer approach discussed above, however, whereas the divide and conquer approach usually implies an approximation, in our method the independent treatment is exact. For all systems studied so far, we could make the total-energy deviation compared to direct solution of (41) as small as we wanted, always smaller than 1 μeV using enough iterations.

4.5 Green Function Truncation

In order to arrive at an $O(N)$ algorithm the nearsightedness of electronic matter[33,34], which is the basis of most other linear-scaling methods, can be used in the following manner. From the relation

$$\rho(\underline{r},\underline{r}',T) = -\frac{2}{\pi}\mathrm{Im}\int_{-\infty}^{\infty} f(E-E_F,T)G(\underline{r},\underline{r}';E)\mathrm{d}E \tag{45}$$

between the finite-temperature density matrix $\rho(\underline{r},\underline{r}',T)$ and the Green function $G(\underline{r},\underline{r}';E)$ and from the property that the Green function decays faster for energies E with larger imaginary part, it can be concluded (via the complex energy contour integration discussed above) that the decay of $\rho(\underline{r},\underline{r}',T)$ is mainly determined by the decay of $G(\underline{r},\underline{r}';E_F+\mathrm{i}\pi kT)$ at the first Matsubara energy. Thus a neglect of the Green function for large distances $|\underline{r}-\underline{r}'|$ corresponds to a neglect of the finite-temperature density matrix for similar distances.

Since the single-scattering wavefunctions in (40) are only multiplicative factors, a truncation of the Green function directly corresponds to a neglect of Green function matrix elements $G_{LL'}^{nn'}$ beyond a chosen distance d_{cut}, which means that in (41) only $O(N_{tr}N_{at})$ elements $G_{LL'}^{nn'}$ are non-zero instead of $O(N_{at}^2)$. This reduces the computational effort by a factor N_{tr}/N_{at} if multiplication with zero elements is avoided by appropriate storage techniques. Here N_{tr} is the number of atoms which are included in the truncation region defined by $|\underline{R}^n - \underline{R}^{n'}| < d_{cut}$. The total effort is then proportional to $N_{it}N_{cl}N_{tr}N_{at}$. This increases linearly with N since the number of atoms N_{at} increases as the number of electrons N and since N_{cl} and N_{tr} are fixed numbers and since N_{it} approaches a constant value for large systems (see next section).

4.6 Iteration Behaviour and Total Energy Results

To illustrate how the calculated total energy is affected by the Green function truncation and how the number of iterations depends on the truncation region, results calculated with our algorithm for a large Ni supercell are shown in Fig. 3. The supercell was constructed by repeating a simple cubic unit cell with four atoms 32 times in all three space directions resulting in a supercell with $4\times 32^3 = 131072$ atoms. The lattice constant a was chosen as 11.276 nm, which is 32 times the experimental lattice constant of Ni. The repulsive muffin-tin potentials in the reference system had a height of 8 Ryd and cluster with $N_{cl} = 13$ atoms

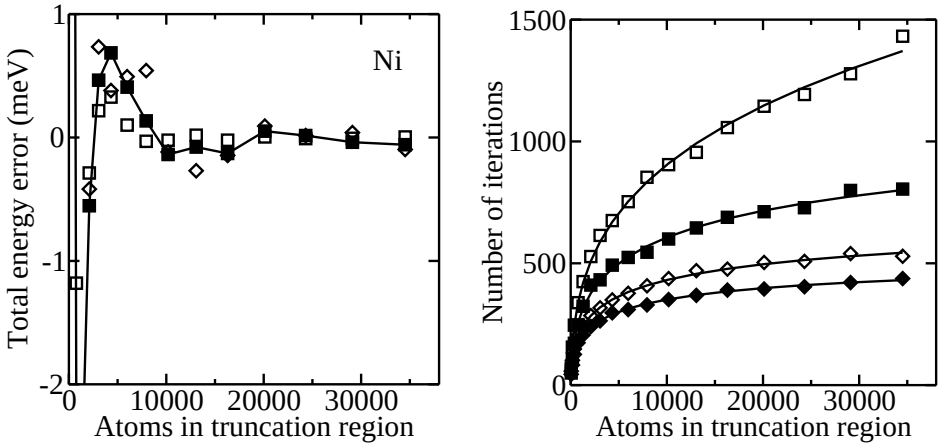

Figure 3. Left picture: Total energy error per atom as function of the number of atoms contained in the truncation region. Solid and open squares are for T = 800 K and 1600 K, diamonds for T = 400 K. The lines, which connect the results for T = 800 K, serve as guide for the eye. Right picture: Number N_{it} of iterations (matrix-vector multiplications averaged over the 16 angular momentum components) as function of the number N_{tr} of atoms contained in the truncation region. The lines are fitted to an exponential behaviour as described in the text. Solid (open) symbols denote results for the majority (minority) spin direction. The squares are for T = 800 K and the diamonds for T = 1600 K.

(central atom and its 12 nearest neighbours) were chosen to calculate the Green function matrix elements (42) of the reference system. A single point $\underline{k} = (1/4, 1/4, 1/4) \times 2\pi/a$ was used in the irreducible part of the Brillouin zone of the supercell. Since all atoms in the supercell are equivalent, the iterative solution of (41) was needed for only one value of n'. This represented an enormous reduction of the computational effort in the present model study compared to realistic systems with inequivalent atoms. Note that for $N_{at} = 131072$ and $l_{max} = 3$ the dimension of the matrices in (41) is $N_{at}(l_{max}+1)^2 = 2097152$ and that the matrix G^r has a sparsity degree of $13/131072 \approx 0.01\%$.

To study the truncation effect on the total energy one needs to know the total energy of Ni supercell calculated without truncation. Since only the density within one cell is required (all cells have the same density), such a calculation is possible with our present computer code. However, without truncation already about 7 Gigabyte are needed to store the non-zero elements of G^r and the self-consistent determination of the effective potential and the total energy would be rather expensive. Here the use of equivalent $\underline{k}$ point meshes[81] for the supercell and the simple cubic unit cell is of great help. If appropriate $\underline{k}$ points are used in the Brillouin zones, the calculated on-site Green function matrix elements for the supercell with equivalent atoms and for the simple cubic cell agree exactly. Thus the self-consistent potential and the correct total energy for the large Ni supercell with the single $\underline{k}$ point could be obtained inexpensively by self-consistent calculations for a simple cubic unit cell with 5984 $\underline{k}$ points.

The truncation regions were constructed by using more and more neighbour shells around the central atom so that always one more shell in the close-packed (110) direction was included. The smallest truncation region with 55 atoms included two neighbours in that direction and the largest truncation region with 34251 atoms included 18 neighbours in

that direction. The calculated total energy error is shown in Table 1 for small and in Fig. 3 for large truncation regions for three different temperatures. Whereas for small truncation regions the error can be as large as 0.1 eV, Fig. 3 shows that the error can be made smaller than 2 meV if truncation regions with a few thousand atoms are used. Since one is usually not interested in absolute total energies, but in total energy differences or derivatives (for instance forces, which can be calculated in the KKR method in a straightforward manner[69,82]), it can be expected that due to cancellation effects truncation regions with about a few hundred atoms are sufficient for the calculation of energy changes and forces with our linear scaling algorithm.

N_{tr}	ΔE_{400}	ΔE_{800}	ΔE_{1600}
55	121.9	135.6	123.2
177	87.3	105.8	125.6
381	33.6	31.0	26.4
767	-9.5	-7.9	-4.0
1289	-11.0	-9.8	-7.1
2093	-1.4	-1.9	-1.0

Table 1. Total energy error (in meV) as function of the number of atoms in the truncation region for three temperatures $T = 400$, 800, and 1600 K.

An important issue for our algorithm is how fast the iterations converge. The main computational work consists in matrix-vector multiplications, which were repeated independently for each angular-momentum component L' until the prescribed precision (specified by the residual norm $||r|| = 10^{-6}$ in the QMR method) were obtained. Fig. 3 shows the number of iterations (averaged over the $(l_{max}+1)^2 = 16$ angular-momentum components) at the first Matsubara energy $E_F + \mathrm{i}\pi kT$ where the slowest convergence exists. The number of iterations increases with increasing truncation region and can be fitted to an exponential behaviour of the form[66,67]

$$N_{it}(N_{tr}) = N_{it}^{\infty} - \alpha \exp(\gamma N_{tr}^{1/3}) \tag{46}$$

with three temperature dependent parameters N_{it}^{∞}, α and γ, which indicates that N_{it} approaches a constant value for large truncation regions. Whereas temperature has a pronounced effect on the computing time (via N_{it}), it seems that higher temperature does not much reduce the truncation error for the total energy, only for regions with more than 10000 atoms a reduction is seen. This probably means that the zero-temperature algebraical decay of the Green function (and density matrix) dominates the additional exponential decay caused by temperature up to truncation distances of approximately 10 times the Ni lattice constant.

Appendix

The expectation values $\langle\Psi|v_{ext}|\Psi\rangle$ and $\langle\Psi|\hat{U}|\Psi\rangle$ can be expressed in terms of the density $n(\underline{r})$ and the pair density $n_2(\underline{r},\underline{r}')$. The density is given by the expectation value of the

density operator $\hat{n}$ as

$$n(\underline{r}) = \langle\Psi|\hat{n}|\Psi\rangle = \int\cdots\int |\Psi(\underline{r}_1,...,\underline{r}_N)|^2 \sum_i^N \delta(\underline{r}-\underline{r}_i)\mathrm{d}\underline{r}_1...\mathrm{d}\underline{r}_N \,. \tag{47}$$

Multiplication with $v_{ext}(\underline{r})$ and integration leads to

$$\begin{aligned}\int n(\underline{r})v_{ext}(\underline{r})\mathrm{d}\underline{r} &= \int\cdots\int |\Psi(\underline{r}_1,...,\underline{r}_N)|^2 \sum_i^N \delta(\underline{r}-\underline{r}_i)v_{ext}(\underline{r}_i)\mathrm{d}\underline{r}_1...\mathrm{d}\underline{r}_N\mathrm{d}\underline{r} \\ &= \int\cdots\int |\Psi(\underline{r}_1,...,\underline{r}_N)|^2 \sum_i^N v_{ext}(\underline{r}_i)\mathrm{d}\underline{r}_1...\mathrm{d}\underline{r}_N \\ &= \langle\Psi|v_{ext}|\Psi\rangle \,.\end{aligned} \tag{48}$$

Here the first line arises by changing the argument in v_{ext} from $\underline{r}$ into $\underline{r}_i$, which is possible because of $\delta(\underline{r}-\underline{r}_i)$, and the second line arises by integration over the δ function. The pair density is given by the expectation value of the two-particle density operator $\hat{n}_2$ as

$$\begin{aligned}n_2(\underline{r},\underline{r}') = \langle\Psi|\hat{n}_2|\Psi\rangle = \int\cdots\int |\Psi(\underline{r}_1,...,\underline{r}_N)|^2 \sum_{i\neq j}^N\sum \delta(\underline{r}-\underline{r}_i)\delta(\underline{r}'-\underline{r}_j) \\ \mathrm{d}\underline{r}_1...\mathrm{d}\underline{r}_N \,.\end{aligned} \tag{49}$$

Proceeding similarly as above leads to

$$\begin{aligned}\int n_2(\underline{r},\underline{r}')U(\underline{r},\underline{r}')\mathrm{d}\underline{r}\mathrm{d}\underline{r}' &= \int\cdots\int |\Psi(\underline{r}_1,...,\underline{r}_N)|^2 \sum_{i\neq j}^N\sum \delta(\underline{r}-\underline{r}_i)\delta(\underline{r}'-\underline{r}_j) \\ &\quad \times U(\underline{r}_i,\underline{r}_j)\mathrm{d}\underline{r}_1...\mathrm{d}\underline{r}_N\mathrm{d}\underline{r}\mathrm{d}\underline{r}' \\ &= \int\cdots\int |\Psi(\underline{r}_1,...,\underline{r}_N)|^2 \sum_{i\neq j}^N\sum U(\underline{r}_i,\underline{r}_j)\mathrm{d}\underline{r}_1...\mathrm{d}\underline{r}_N \\ &= 2\int\cdots\int |\Psi(\underline{r}_1,...,\underline{r}_N)|^2 \sum_{i<j}^N\sum U(\underline{r}_i,\underline{r}_j)\mathrm{d}\underline{r}_1...\mathrm{d}\underline{r}_N \\ &= 2\langle\Psi|\hat{U}|\Psi\rangle \,,\end{aligned} \tag{50}$$

where the double sum over $i \neq j$ has been has replaced by twice the double sum over $i < j$. Note that the approximation $n_2(\underline{r},\underline{r}') = n(\underline{r})n(\underline{r}')$ leads to the expression of the electron-electron interaction used in (14) and the pair density must be distinguished one-particle density matrix defined as

$$\rho(\underline{r},\underline{r}') = N\int\cdots\int \Psi^\star(\underline{r},\underline{r}'_2,...,\underline{r}_N)\Psi(\underline{r}',\underline{r}'_2,...,\underline{r}_N)\mathrm{d}\underline{r}_2...\mathrm{d}\underline{r}_N \,. \tag{51}$$

References

1. L. H. Thomas, *The calculation of atomic fields*, Proc. Cambridge Philos. Soc. **23**, 542-548, 1927
2. E. Fermi, *Un metodo statistico per la determinazione di alcune proprietà dell'atomo*, Atti Accad, Naz. Lincei, Cl. Sci. Fis. Mat. Nat. Rend. **6**, 602–607, 1927.
3. P. Hohenberg and W. Kohn, *Inhomogeneous Electron Gas*, Phys. Rev. **136**, B864–B871, 1964.
4. R. Evans, Adv. Phys. **28**, 143–200 (1979) and in *Fundamentals of Inhomogeneous Fluids*, ed. by D. Hendersen (Dekker, New York, 1992).
5. M. Brack in *Density Functional Methods in Physics*, NATO ASI Series B, Vol. 123 (Plenum Press, New York, 1985).
6. R. Zeller, *Introduction to Density-Functional Theory*, in Computational Condensed Matter Physics, Lecture Manuscripts of the 37^{th} Spring School of the Institute of Solid State Research, S. Blügel, G. Gompper, E. Koch, H. Müller-Krumbhaar, R. Spatschek, R .G. Winkler (Eds.), Forschungszentrum Jülich GmbH, A1.1-A1.19, 2006.
7. E. H. Lieb, *Density Functionals for Coulomb Systems*, Int. J. Quant. Chem. **24**, 243–277, 1983
8. M. Reed and B. Simon, *Methods of Modern Mathematical Physics*, (Academic, New York, 1978),Vol. **4**.
9. W. Kohn and L. J. Sham, *Self-Consistent Equations Including Exchange and Correlation Effects*, Phys. Rev. **140**, A1133–A1138, 1965.
10. M. Levy, *Universal variational functionals of electron densities, first-order density matrices, and natural spin-orbitals and solution of the v-representability problem*, Proc. Natl. Acad. Sci. U. S. A. **76**, 6062–6065, 1979.
11. V. Eyert, *A Comparative Study on Methods for Convergence Acceleration of Iterative Vector Sequences*, J. Comput. Phys. **124**, 271-285, 1996.
12. P. H. Dederichs and R. Zeller, *Self-consistency iterations in electronic-structure calculations*, Phys. Rev. B **28**, 5462, 1983.
13. D. M. Ceperly and B. J. Alder, *Ground State of the Electron Gas by a Stochastic Method*, Phys. Rev. Lett. **45**, 566–569, 1980.
14. S. H. Vosko, L. Wilk, and M. Nusair, *Accurate spin-dependent electron liquid correlation energies for local spin density calculations: a critical analysis*, Can. J. Phys. **58**, 1200–1211, 1980.
15. J. P. Perdew and A. Zunger, *Self-interaction correction to density functional approximations for many-electron systems*, Phys. Rev. B **23**, 5048–5079, 1981.
16. A. D. Becke, *Density-functional exchange-energy approximation with correct asymptotic behavior*, Phys. Rev. A **38**, 3098-3100, 1988.
17. J. P. Perdew, J. A. Chevary, S. H. Vosko, K. A. Jackson, M. R. Pederson, D. J. Singh, and C. Fiolhais, *Atoms, molecules, solids, and surfaces: Applications of the generalized gradient approximation for exchange and correlation*, Phys. Rev. B **46**, 6671–6687, 1992; *Erratum*, Phys. Rev. B **48**, 4978, 1993.
18. J. P. Perdew, K. Burke, and M. Ernzerhof, *Generalized Gradient Approximation Made Simple*, Phys. Rev. Lett. **77**, 3865–3868, 1996.

19. J. P. Perdew, S. Kurth, A. Zupan, and P. Blaha, *Accurate Density Functional with Correct Formal Properties: A Step Beyond the Generalized Gradient Approximation*, Phys. Rev. Lett. **82**, 2544–2547, 1999.
20. J. Tao, J. P. Perdew, V. N. Staroverov, and G. E. Scuseria, *Climbing the Density Functional Ladder: Nonempirical MetaGeneralized Gradient Approximation Designed for Molecules and Solids*, Phys. Rev. Lett. **91**, 146401-1–4, 2003.
21. V. I. Anisimov, J. Zaanen, and O. K. Andersen, *Band theory and Mott insulators: Hubbard U instead of Stoner I*, Phys. Rev. B **44**, 943–954, 1991.
22. S. Kümmel and L. Kronik, *Orbital-dependent density functionals: theory and applications*, Rev. Mod. Phys **80**, 3–60, 2008.
23. A. D. Becke, *A new mixing of Hartree-Fock and local density-functional theories*, J. Chem. Phys. **98**, 1372–1377, 1993.
24. A. D. Becke, *Density-functional thermochemistry. III. The role of exact exchange*, J. Chem. Phys. **98**, 5648–5652, 1993.
25. C. Lee, W. Yang, and R. G. Parr, *Development of the Colle-Salvetti correlation-energy formula into a functional of the electron density*, Phys. Rev. B **37**, 785–789, 1988.
26. O. K. Andersen, *Linear methods in band theory*, Phys. Rev. B **12**, 3060–3083, 1975.
27. J. R. Chelikowsky, N. Troullier, and Y. Saad, *Finite-difference-pseudopotential method: Electronic structure calculations without a basis*, Phys. Rev. Lett. **72**, 1240–1243, 1994.
28. S. R. White, J. W. Wilkins, and M. P. Teter, *Finite-element method for electronic structure*, Phys. Rev. B **39**, 5819–5833, 1989.
29. E. L. Briggs, D. J. Sullivan, and J. Bernholc, *Large-scale electronic-structure calculations with multigrid acceleration*, Phys. Rev. B **52**, R5471–R5474, 1995.
30. T. L. Beck, K. A. Iyer, and M. P. Merrick, *Multigrid methods in density functional theory*, Int. J. Quant. Chem. **341–348**, 1997, .
31. K. Cho, T. A. Arias, J. D. Joannopoulos, and P. K. Lam, *Wavelets in electronic structure calculations*, Phys. Rev. Lett. **71**, 1808–1811, 1993.
32. S. Wei and M. Y. Chou, *Wavelets in Self-Consistent Electronic Structure Calculations*, Phys. Rev. Lett. **76**, 2650–2653, 1996.
33. E. Prodan and W. Kohn, *Nearsightedness of electronic matter*, Proc. Natl. Acad. Sci. USA **102**, 11635–11638, 2005.
34. W. Kohn, *Density Functional and Density Matrix Method Scaling Linearly with the Number of Atoms*, Phys. Rev. Lett. **76**, 3168–3171, 1996.
35. T. L. Beck, *Real-space mesh techniques in density-functional theory*, Rev. Mod. Phys. **72**, 1041–1080, 2000.
36. T. A. Arias, *Multiresolution analysis of electronic structure: semicardinal and wavelet bases*, Rev. Mod. Phys. **71**, 267–311, 1999.
37. S. Goedecker, *Decay properties of the finite-temperature density matrix in metals*, Phys. Rev. B **58**, 3501–3502, 1998.
38. S. Ismail-Beigi and T. A. Arias, *Locality of the Density Matrix in Metals, Semiconductors, and Insulators*, Phys. Rev. Lett. **82**, 2127–2130, 1999.
39. S. Goedecker, *Linear scaling electronic structure methods*, Rev. Mod. Phys. **71**, 1085–1123, 1999.
40. W. Yang, *Direct calculation of electron density in density-functional theory*, Phys. Rev. Lett. **66**, 1438–1441, 1991.

41. Y. Wang, G. M. Stocks, W. A. Shelton, D. M. Nicholson, Z. Szotek, and W. M. Temmerman, *Order-N Multiple Scattering Approach to Electronic Structure Calculations*, Phys. Rev. Lett. **75**, 2867–2870, 1995.
42. I. A. Abrikosov, A. M. Niklasson, S. I. Simak, B. Johansson, A. V. Ruban, and H. L. Skriver, *Order-N Green's Function Technique for Local Environment Effects in Alloys*, Phys. Rev. Lett. **76**, 4203–4206, 1996.
43. I. A. Abrikosov, S. I. Simak, B. Johansson, A. V. Ruban, and H. L. Skriver, *Locally self-consistent Green's function approach to the electronic structure problem*, Phys. Rev. B **56**, 9319–9334, 1983.
44. A. V. Smirnov and D. D. Johnson, *Accuracy and limitations of localized Green's function methods for materials science applications*, Phys. Rev. B **64**, 235129-1–9, 2001.
45. S. Goedecker and L. Colombo, *Efficient Linear Scaling Algorithm for Tight-Binding Molecular Dynamics*, Phys. Rev. Lett. **73**, 122–125, 1993.
46. A. F. Voter, J. D. Kress, and R. N. Silver, *Linear-scaling tight binding from a truncated-moment approach*, Phys. Rev. B **53**, 12733–12741, 1996.
47. R. Haydock, V. Heine, and M. J. Kelly, *Electronic structure based on the local atomic environment for tight-binding bands*, J. Phys. C **5**, 2845–2858, 1972.
48. R. Haydock, V. Heine, and M. J. Kelly, *Electronic structure based on the local atomic environment for tight-binding bands. II*, J. Phys. C **8**, 2591–2605, 1975.
49. `http://www.openmx-square.org/`
50. T. Ozaki and H. Kino, *Efficient projector expansion for the ab initio LCAO method*, Phys. Rev. B **72**, 045121-1–8, 2005.
51. T. Ozaki, *O(N) Krylov-subspace method for large-scale electronic structure calculations*, Phys. Rev. B **74**, 245101-1–15, 2005.
52. X.-P. Li, R. W. Nunes, and D. Vanderbilt, *Density-matrix electronic-structure method with linear system-size scaling*, Phys. Rev. B **47**, 10891–10894, 1993.
53. M. S. Daw, *Model for energetics of solids based on the density matrix*, Phys. Rev. B **47**, 10895–10898, 1993.
54. E. Hernández and M. J. Gillan, *Self-consistent first-principles technique with linear scaling*, Phys. Rev. B **51**, 10157–10160, 1995.
55. R. Mc Weeny, *Some Recent Advances in Density Matrix Theory*, Rev. Mod. Phys. **32**, 335–369, 1960.
56. `http://www.conquest.ucl.ac.uk/index.html`
57. `http://www2.tcm.phy.cam.ac.uk/onetep/`
58. D. R. Bowler, T. Miyazaki, and M. J. Gillan, *Recent progress in linear scaling ab initio electronic structure techniques*, J. Phys.: Condens. Matter **14**, 2781–2798, 2002.
59. C-K. Skylaris, P. D. Haynes, A. A. Mostofi, and M. C. Payne, *Introducing ONETEP: Linear-scaling density functional simulations on parallel computers*, J. Chem. Phys. **122**, 084119-1–10, 2005.
60. C-K. Skylaris, P. D. Haynes, A. A. Mostofi, and M. C. Payne, *Using ONETEP for accurate and efficient $O(N)$ density functional calculations*, J. Phys.: Condens. Matter **17**, 5757–5769, 2005.
61. F. Mauri, G. Galli, and R. Car, *Orbital formulation for electronic-structure calculations with linear system-size scaling*, Phys. Rev. B **47**, 9973–9976, 1993.

62. P. Ordejón, D. A. Drabold, M. P. Grumbach, and R. M. Martin, *Unconstrained minimization approach for electronic computations that scales linearly with system size*, Phys. Rev. B **48**, 14646–14649, 1993.
63. J. Kim, F. Mauri, and G. Galli, *Total-energy global optimizations using nonorthogonal localized orbitals*, Phys. Rev. B **52**, 1640–1648, 1995.
64. J. M. Soler, E. Artacho, J. D. Gale, A. Garcia, J. Junquera, P. Ordejón, and D. Sanchez-Portal, *The SIESTA method for ab initio order-N materials simulation*, J. Phys.: Condens. Matter **14**, 2745–2779, 2002.
65. `http://www.uam.es/departamentos/ciencias/fismateriac/siesta/`
66. R. Zeller, *Towards a linear-scaling algorithm for electronic structure calculations with the tight-binding Korringa-Kohn-Rostoker Green function method*, J. Phys.: Condens. Matter **20**, 294215-1–8, 2008.
67. R. Zeller, *Linear-scaling total-energy calculations with the tight-binding Korringa-Kohn-Rostoker Green function method*, Phil. Mag. **88**, 2807–2815, 2008.
68. R. Zeller, P. H. Dederichs, B. Újfalussy, L. Szunyogh, and P. Weinberger, *Theory and convergence properties of the screened Korringa-Kohn-Rostoker method*, Phys. Rev. B **52**, 8807–8812, 1995.
69. N. Papanikolaou, R. Zeller, and P. H. Dederichs, *Conceptual improvements of the KKR method*, J. Phys.: Condensed Matter **16**, 2799–2823, 2002.
70. R. Zeller and P. H. Dederichs, *Electronic Structure of Impurities in Cu, Calculated Self-Consistently by Korringa-Kohn-Rostoker Green's-Function Method*, Phys. Rev. Lett. **42**, 1713–1716, 1979.
71. R. Podloucky, R. Zeller, and P. H. Dederichs, *Electronic structure of magnetic impurities calculated from first principles*, Phys. Rev. B **22**, 5777–5790, 1980.
72. O. Gunnarsson, O. Jepsen, and O. K. Andersen, *Self-consistent impurity calculations in the atomic-spheres approximation*, Phys. Rev. B **27**, 7144–7168, 1983.
73. R. Zeller, *Multiple-scattering solution of Schrödinger's equation for potentials of general shape*, J. Phys. C: Solid State Phys. **20**, 2347–2360, 1987.
74. B. Drittler, M. Weinert, R. Zeller, and P. H. Dederichs, *Vacancy formation energies of fcc transition metals calculated by a full potential Green's function method*, Solid State Commun. **79**, 31–35, 1991.
75. R. Zeller, J. Deutz, and P. H. Dederichs, *Application of the complex energy integration to selfconsistent electronic structure calculations*, Solid State Commun. **44**, 993–997, 1982.
76. N. D. Mermin, *Thermal Properties of the Inhomogeneous Electron Gas*, Phys. Rev. **137**, A1441–A1443, 1965.
77. K. Wildberger, P. Lang, R. Zeller, and P. H. Dederichs, *Fermi-Dirac distribution in ab initio Green's-function calculations*, Phys. Rev. B **52**, 11502–11508, 1995.
78. D. G. Anderson, *Iterative Procedures for Nonlinear Integral Equations*, J. Assoc. Comput. Mach. **12**, 547-560, 1965.
79. R. W. Freund and N. M. Nachtigal, *QMR: a quasi-minimal residual method for non-Hermitian linear systems*, Numer. Math **60**, 315–339, 1991.
80. R. W. Freund, *A Transpose-Free Quasi-Minimal Residual Algorithm for Non-Hermitian Linear Systems*, SIAM J. Sci. Comput. **14**, 470–482, 1993.
81. N. Chetty, M. Weinert, T. S. Rahman, and J. W. Davenport, *Vacancies and impurities in aluminum and magnesium*, Phys. Rev. B **52**, 6313–6326, 1995.

82. N. Papanikolaou, R. Zeller, P. H. Dederichs, and N. Stefanou, *Lattice distortion in Cu-based dilute alloys: A first-principles study by the KKR Green-function method*, Phys. Rev. B **55**, 4157–4167, 1997.